JOURNAL OF SOLID STATE CHEMISTRY **47**, 333–349 (1983)

Aluminum Distribution in the Boron Framework of γ-AlB_{12}

IWAMI HIGASHI

The Institute of Physical and Chemical Research, Wako-Shi,
Saitama 351, Japan

Received August 19, 1982

The crystal structure of γ-AlB_{12} ($P2_12_12_1$; $a = 16.573(4)$, $b = 17.510(3)$, $c = 10.144(1)$ Å) was reinvestigated by single-crystal X-ray diffractometry and the nature of the metal distribution in the boron framework examined. Starting from the structure data published by Hughes *et al.* (Journal of the American Chemical Society **83**, 2337 (1977)), 458 independent parameters, including the occupancies of 11 Al sites, were finally refined to a conventional R value of 2.9%. A total of 5282 observed unique reflections (Mo$K\alpha$ radiation; $2\theta < 64°$) were used. Although distributed in an apparently complicated manner, the aluminum atoms occur in the boron framework according to a simple rule as in the crystals of the α-AlB_{12} structure type. The numbers of the valence electrons of Al, allotted to the six boron subunits, B_{12}(i–iv), B_{20}-(C_2,C_s), proportionately to the contact frequencies of Al with the units, are 2.2, 1.9, 2.2, 1.9, 5.3, and 5.2, respectively. The charge assignment is compatible with the ionic formula 20/3 $Al^{+3} \cdot 4B_{12}^{-2} \cdot 2B_{20}^{-6}$, proposed from preliminary molecular orbital calculations. A negative charge balance among the six boron units at about 1 : 1 : 1 : 1 : 3 : 3 seems to be essential for making up the stable boron framework of γ-AlB_{12}.

Introduction

In the course of recent work concerned with the crystallization of boron-rich phases, we obtained crystals of γ-AlB_{12} from high temperature Al–B melts (*1*). The crystals were quite different in crystal shape (*1*) from those reported until now (*2–4*), and had no trace of intergrown α-AlB_{12}; it is very difficult to synthesize γ-AlB_{12} crystals that are completely free from syntactically intergrown α-AlB_{12} (*5*). Furthermore, the lattice constants (space group $P2_12_12_1$; $a = 16.573(4)$, $b = 17.510(3)$, $c = 10.144(1)$ Å) were noticeably shorter than those ($a = 16.623(5)$, $b = 17.540(5)$, $c = 10.180(5)$ Å) observed for the same phase by Hughes *et al.* (*6*). Because of these different characteristics, we undertook the investigation of the crystal structure by single-crystal X-ray diffractometry (*1*). It was refined starting with the structure of a γ-AlB_{12} phase published by Hughes *et al.* (*6*), and accurate structural data were obtained including the occupational parameters of Al sites which were significantly different from the published data. In the present work, therefore, the nature of the metal distribution was examined based on the idea of "charge balance" among boron polyhedral structural subunits; the idea had been introduced to interpret the common nature of the metal distribution in the crystals of α-AlB_{12} structure type (*7*). This paper reports the results of the examination, together with some structural details, most of which have not been described in the previous papers (*1, 6*).

0022-4596/83 $3.00

TABLE I

CRYSTAL AND INTENSITY MEASUREMENT DATA

Space group	$P2_12_12_1$
a(Å)	16.573(4)
b(Å)	17.510(3)
c(Å)	10.144(1)
Formula unit[a]	$B_{88}Al_{6.3}$
D_m(g/cm³)[b]	2.5
D_x(g/cm³)	2.53
Z	4
μ for Mo$K\alpha$ (cm⁻¹)	2.8
Crystal dimensions (mm)	0.40 × 0.30 × 0.25
Reflections measured	$0 \leq h \leq 24$ $0 \leq k \leq 26$ $0 \leq l \leq 15$
$2\theta_{\max}$(°)	64
Number of independent reflections collected	5282

[a] The asymmetric unit determined by the present structure analysis.

[b] Flotation in a mixture of tribromomethane and acetone.

Intensity Measurement

The method of the preparation of the crystals is described in a previous paper (*1*). A well-formed hexagonal columnar crystal was selected for the X-ray diffraction work. The lattice constants were determined from 20 reflections in the 2θ range of 57–64°. These were measured with the same diffractometer used for the intensity data collection; the wavelength employed was 0.70930 Å for Mo$K\alpha_1$. The reflections were collected on a Rigaku automated four-circle diffractometer, with Mo$K\alpha$ radiation monochromated with a graphite monochrometer. A 2θ-ω scan mode at a rate of 2° (in ω)/min was used. The background counts of 5 sec were measured on each side of the scanning width ($\Delta\theta = 1 + 0.5 \tan \theta$). Three standard reflections were monitored for every 100 reflections; no significant variations were observed. The intensities were corrected for the Lorentz and polarization effects. No absorption or extinction[1] corrections were made. A total of 5282 independent reflections with F_o values greater than 2.5 times the standard deviations was used in the structure analysis. Crystal and intensity measurement data are summarized in Table I.

Refinement of the Structure

As referred to in the Introduction, the structure of the present crystal was refined starting with the structural parameters of γ-AlB_{12} which had been published by Hughes *et al.* ($R = \Sigma|F_o| - |F_c|)/\Sigma|F_o| = 0.059$; $R_w = (\Sigma w(|F_o| - |F_c|)^2/\Sigma w|F_o|^2)^{1/2} = 0.078$, w = unit weight; 5439 observed reflections). The published structure with 427 independent parameters is summarized as follows. The boron framework of γ-AlB_{12} consists of four crystallographically independent B_{12} icosahedra and two kinds of B_{20} units (Fig. 1). One of the B_{20} units, B_{20}-(C_2), is the same as that found in α-AlB_{12} (*8*, *9*) and $Al_{\sim1.1}Be_{\sim0.6}B_{22}$ (*7*), and the other, B_{20}-(C_s), is the one that has been found only in γ-AlB_{12} (*6*); each of the symbols characterizes the symmetry of the respective unit in the standard Schoenflies notation (*6*). The Al atoms are distributed over eight sites, Al(1)–Al(8), which are present outside the boron structural subunits. Of these sites, Al(7) and Al(8) are partially filled, with occupancies of 0.536(6) and 0.431(6), respectively.

For the structure refinement of the present crystal, block-diagonal least-squares and difference Fourier methods were used. The atomic scattering factors were taken from the International Tables for X-ray Crystallography (1974) (*10*). All the calculations for the structure analysis

---

[1] Extinction effects were not noticeable in the final F_o-F_c table; the discrepancies between the observed and calculated structure factors $2(F_o\text{-}F_c)/(F_o + F_c)$ of the five strongest lower angle reflections ($\sin \theta/\lambda < 0.3$) were in the range −0.9–+2.2%, showing no systematic trend.

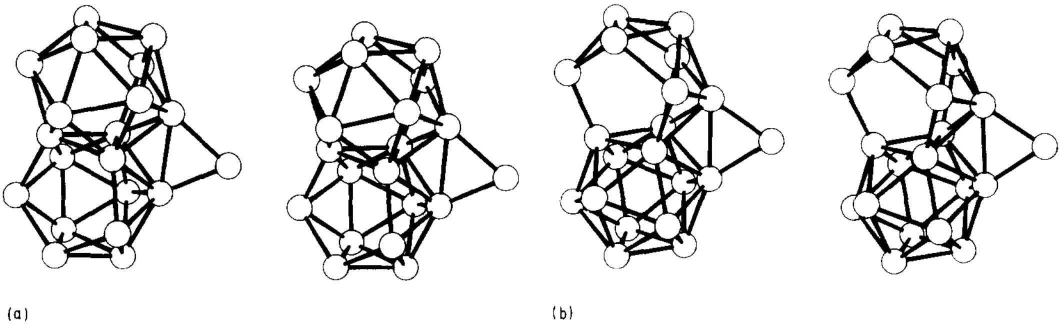

FIG. 1. Stereoscopic views of (a) B_{20}-(C_2) and (b) B_{20}-(C_s) units.

were made with the aid of the program UNICS-III (*11*) on the FACOM M200 computer installed in this institute. A preliminary refinement of the structure of the present crystal was made starting from all the published parameters. Anisotropic temperature factors were applied to the Al sites. The function minimized in the refinement was $\Sigma w(|F_o| - |F_c|)^2$, with unit value for every weight w. The refinement converged at $R = 0.060$ *and* $R_w = 0.070$, resulting in the occupancies 0.96, 0.96, 0.96, 0.53, 0.77, 0.77, 0.49, and 0.47 for the metal sites Al(1)–Al(8), respectively. A difference synthesis calculated subsequently, however, showed three additional maxima, two of which exhibited considerably high intensities. These three sites were assigned as Al sites, Al(9,10,11), because their distances from surrounding boron atoms were in the range of 2.0 to 3.0 Å in accordance with Al–B bond lengths in α-AlB$_{12}$ (*8*) and Al$_{\sim1.1}$Be$_{\sim0.6}$B$_{22}$ (*7*). Adding the three Al sites, the refinements of 458 independent parameters were finally made including the occupancies of the new sites. Anisotropic temperature factors were applied to all the Al sites but Al(11) which had exceptionally low occupancy. In this final cycle of refinement the weight was chosen as $w = [\sigma(F_o)]^{-2}$ for every reflection. The $R(Rw)$ value obtained was 0.029 (0.036). The difference synthesis finally calculated showed no more maxima exceeding 0.5 e Å^{-3}. The final structural parameters of the boron and Al atoms are presented in Table II and Table III, respectively. The listing of atoms in Tables II and III follows that given by Hughes *et al.* The Roman characters i, ii, iii, iv, v, and vi in the boron atom designations refer to the boron polyhedral units to which these atoms belong. Characters i, ii, iii, and iv indicate atoms in the four crystallographically independent icosahedra. The character v refers to atoms in the B_{20}-(C_2) unit and the character vi indicates atoms in the B_{20}-(C_s) units. Observed and calculated structure factors (Table IV) are presented in a separate table.[2] The B–B bond lengths are given in Table V.

Results and Discussions

The Structure of the Boron Framework

The boron framework of the present crystal is identical with that reported by Hughes *et al.* It was succinctly described

---

[2] See NAPS document No. 04075 for 54 pages of supplementary material. Order from ASIS/NAPS, Microfiche Publications, P.O. Box 3513, Grand Central Station, New York, NY 10163. Remit in advance \$4.00 for microfiche copy or for photocopy, \$17.95 up to 20 pages plus \$.30 for each additional page. All orders must be prepaid. Institutions and organizations may order by purchase order. However, there is a billing and handling charge for this service of \$15. Foreign orders add \$4.50 for postage and handling, for the first 20 pages, and \$1.00 for additional 10 pages of material. Remit \$1.50 for postage of any microfiche orders.

TABLE II

Atomic Coordinates ($\times 10^4$)[a] and Temperature Factors for Boron Sites in γ-AlB$_{12}$

Atom	x	y	z	B(Å^2)	Atom	x	y	z	B(Å^2)
Bi(1)	1830	2082	105	0.38	Biv(9)	5676	2391	−3636	0.45
Bi(2)	1855	2920	1138	0.39	Biv(10)	5821	1384	−3738	0.43
Bi(3)	1746	3047	−647	0.37	Biv(11)	4781	943	−3703	0.41
Bi(4)	2338	2312	−1451	0.41	Biv(12)	4948	1782	−4560	0.41
Bi(5)	2594	2151	1411	0.40	Bv(1)	2704	3890	4180	0.42
Bi(6)	2817	1768	−245	0.38	Bv(2)	3247	4713	4802	0.39
Bi(7)	2420	3654	252	0.43	Bv(3)	1749	6211	717	0.43
Bi(8)	2686	3282	−1411	0.42	Bv(4)	3286	3510	2904	0.41
Bi(9)	2943	3110	1467	0.45	Bv(5)	3294	4548	3117	0.43
Bi(10)	3485	2381	585	0.37	Bv(6)	4202	4826	4021	0.41
Bi(11)	3384	2474	−1131	0.37	Bv(7)	831	5636	630	0.45
Bi(12)	3442	3285	−113	0.41	Bv(8)	825	6671	474	0.44
Bii(1)	4362	3747	−147	0.38	Bv(9)	4197	3173	3633	0.43
Bii(2)	5223	3454	−1135	0.40	Bv(10)	4211	4040	2826	0.44
Bii(3)	5198	3294	629	0.40	Bv(11)	4777	3892	4365	0.42
Bii(4)	4708	4084	1415	0.42	Bv(12)	1663	3981	4559	0.43
Bii(5)	4733	4404	−1442	0.43	Bv(13)	2699	6638	586	0.46
Bii(6)	4396	4727	204	0.36	Bv(14)	2409	6102	2099	0.44
Bii(7)	6084	3621	−124	0.37	Bv(15)	1802	5273	1570	0.56
Bii(8)	5772	4014	1447	0.36	Bv(16)	2417	4645	527	0.44
Bii(9)	5842	4324	−1423	0.40	Bv(17)	3397	5966	1306	0.41
Bii(10)	5321	5100	−592	0.40	Bv(18)	2890	5117	1913	0.48
Bii(11)	5276	4927	1125	0.40	Bv(19)	3436	5129	404	0.45
Bii(12)	6161	4659	234	0.43	Bv(20)	761	5107	2133	0.49
Biii(1)	4936	1656	3796	0.37	Bvi(1)	3495	−557	846	0.42
Biii(2)	4799	767	2926	0.40	Bvi(2)	2540	−781	181	0.39
Biii(3)	5779	1235	2931	0.34	Bvi(3)	3503	−1035	−686	0.43
Biii(4)	5618	2229	2880	0.36	Bvi(4)	3691	−1206	2136	0.39
Biii(5)	4024	1532	2784	0.44	Bvi(5)	2655	−878	1868	0.37
Biii(6)	4584	2407	2825	0.40	Bvi(6)	2099	−1603	952	0.42
Biii(7)	5418	786	1472	0.42	Bvi(7)	2644	−1690	−657	0.40
Biii(8)	5903	1722	1412	0.44	Bvi(8)	3697	−2024	−412	0.38
Biii(9)	4345	1008	1360	0.40	Bvi(9)	4202	8714	599	0.41
Biii(10)	4240	2006	1328	0.35	Bvi(10)	3805	−2129	1351	0.36
Biii(11)	5161	2450	1351	0.39	Bvi(11)	2872	−1877	2150	0.38
Biii(12)	5041	1599	457	0.39	Bvi(12)	2860	−2394	639	0.45
Biv(1)	5038	1696	−1218	0.39	Bvi(13)	3735	389	486	0.42
Biv(2)	5176	2617	−2060	0.45	Bvi(14)	2849	−26	4428	0.39
Biv(3)	4184	2163	−2051	0.36	Bvi(15)	2569	−715	−1610	0.49
Biv(4)	4333	1142	−2158	0.41	Bvi(16)	3575	−450	−2106	0.44
Biv(5)	5951	1879	−2137	0.41	Bvi(17)	2946	788	−431	0.35
Biv(6)	5423	934	−2309	0.40	Bvi(18)	2782	321	−1952	0.47
Biv(7)	4585	2576	−3568	0.42	Bvi(19)	3769	466	−1325	0.45
Biv(8)	4019	1680	−3593	0.42	Bvi(20)	2090	−1571	−2144	0.44

---

[a] The standard deviations of the atomic coordinates are ±0.0001, ±0.0001 and ±0.0002 for every x, y, and z, respectively.

TABLE III

ATOMIC COORDINATES ($\times 10^5$), TEMPERATURE FACTORS,[a] AND OCCUPANCIES FOR ALUMINUM SITES IN γ-AlB$_{12}$

Atom	x	y	z	U_{11}	U_{22}	U_{33}	U_{12}	U_{13}	U_{23}	B_{eq}(Å^2)	Occupancy
Al(1)	21952(4)	9530(4)	11911(7)	65(3)	61(3)	44(3)	−4(2)	2(2)	4(2)	0.45	0.961(4)
Al(2)	36465(4)	1482(4)	26252(7)	47(3)	96(3)	37(3)	−21(2)	−3(2)	6(2)	0.48	0.953(4)
Al(3)	548(4)	95902(5)	45179(7)	44(3)	159(4)	43(3)	23(3)	−2(2)	−12(3)	0.65	0.946(4)
Al(4)	2749(8)	13059(8)	33520(13)	89(6)	92(6)	58(6)	36(5)	17(5)	23(5)	0.63	0.523(4)
Al(5)	19779(6)	39727(6)	23828(9)	121(5)	95(4)	40(4)	−47(3)	4(3)	−8(3)	0.68	0.747(4)
Al(6)	16466(5)	56113(5)	37977(9)	89(4)	58(4)	50(4)	−16(3)	15(3)	1(3)	0.52	0.764(4)
Al(7)	36470(12)	22481(9)	44874(16)	353(10)	129(7)	104(7)	−168(7)	130(7)	−43(6)	1.54	0.511(4)
Al(8)	32891(11)	25394(10)	44075(18)	128(8)	160(8)	127(8)	−109(6)	7(6)	35(6)	1.09	0.444(4)
Al(9)	20803(22)	28787(21)	33000(37)	54(16)	65(16)	62(16)	−32(12)	3(12)	17(12)	0.48	0.188(4)
Al(10)	20200(24)	50484(27)	35717(40)	99(18)	266(23)	79(19)	34(15)	36(14)	89(16)	1.17	0.190(4)
Al(11)	9956(54)	65608(51)	27326(92)							0.2(2)	0.068(4)

[a] The expression of the anisotropic temperature factors is $\exp\{-10^{-4}\cdot 2\pi^2(U_{11}h^2a^{*2} + U_{22}k^2b^{*} + U_{33}l^2c^{*2} + 2U_{12}hka^{*}b^{*} + 2U_{13}hla^{*}c^{*} + 2U_{23}klb^{*}c^{*})\}$. Equivalent isotropic temperature factors are calculated from the relation $B_{eq} = 8/3\,\pi^2\Sigma_i\Sigma_j U_{ij}a_i^{*}a_j^{*}\mathbf{a}_i\cdot\mathbf{a}_j$. For the Al(11) site, conventional isotropic temperature factor is given.

by them by introducing a structural subunit B$_{48}$-(T$_d$) made up of four B$_{12}$ icosahedra. According to the description, the bilayered sheet of icosahedra comprised of a kagomé layer of interconnected B$_{48}$-(T$_d$) units is the basic structural layer in the framework of γ-AlB$_{12}$. The B$_{48}$-(T$_d$) is composed of the four crystallographically independent B$_{12}$ icosahedra. Hughes *et al.* also indicated that the B$_{12}$ icosahedral framework of γ-AlB$_{12}$ is describable with another structural subunit, B$_{144}$-(T$_d$), in which 12 interbonded icosahedra define the vertices of a regular truncated tetrahedron. The B$_{20}$-(C$_2$) and B$_{20}$-(C$_s$) units fill the large holes inside the B$_{144}$-(T$_d$) units.

It is of interest in the present work to determine the nature of the metal distribution among B$_{12}$ icosahedra and B$_{20}$ units. Structural details will be described and discussed by reducing the B$_{48}$-(T$_d$) unit into B$_{12}$(i), B$_{12}$(ii), B$_{12}$(iii), and B$_{12}$(iv). Figure 2 shows B$_{12}$ icosahedral arrangement as seen along the *a* axis, which deviates noticeably from the arrangement of ideal B$_{48}$-(T$_d$) models (*6*). The full structure of B$_{12}$ icosahedral network, which consists of the above mentioned bilayered sheet of icosahedra (*6*), is obtainable with operating 2$_1$ symmetry operators as indicated in the figure. Thus, the structure has B$_{48}$-(T$_d$) subunits which are piled up infinitely along the *a* axis. Figure 3 shows the feature of such a construction; it was drawn schematically, connecting circles about the centers of the icosahedra. The large openings around each of the B$_{48}$-(T$_d$) subunits are holes inside the B$_{144}$-(T$_d$)—truncated tetrahedra with 12 B$_{12}$ icosahedra at their respective apical sites. Crystallographically, there are two kinds of such polyhedra; one accommodates a B$_{20}$-(C$_2$) unit and the other a B$_{20}$-(C$_s$) unit. As seen from the figure, every B$_{144}$-(T$_d$) truncated tetrahedron is placed so as to have its one hexagonal plane and the opposite triangular plane approximately parallel to the *bc* plane. These two planes and three hexagonal planes of the truncated tetrahedron are shared with similar neighboring polyhedra, and the remaining three triangular planes are shared with three adjacent B$_{48}$-(T$_d$) tetrahedra. Thus, the B$_{12}$ icosahedral arrangement of γ-AlB$_{12}$ is regarded as a structure completely filled with both B$_{48}$-(T$_d$) tetrahedra and B$_{144}$-(T$_d$) truncated tetrahedra, every plane of which is shared with a neighboring tetrahedron or a truncated tetrahedron.

Figure 4 shows the arrangement of B$_{20}$-(C$_2$) and B$_{20}$-(C$_s$) units as seen along the

TABLE V

B–B DISTANCES IN γ-AlB_{12} (Å)

B–B bond lengths within B_{12}(i) icosahedron

Bi(1)–Bi(2)	1.803(3)	Bi(3)–Bi(7)	1.791(3)	Bi(7)–Bi(8)	1.861(3)
–Bi(3)	1.859(3)	–Bi(8)	1.788(3)	–Bi(9)	1.782(3)
–Bi(4)	1.834(3)	Bi(4)–Bi(6)	1.742(3)	–Bi(12)	1.850(3)
–Bi(5)	1.836(3)	–Bi(8)	1.793(3)	Bi(8)–Bi(11)	1.848(3)
–Bi(6)	1.762(3)	–Bi(11)	1.785(3)	–Bi(12)	1.817(3)
Bi(2)–Bi(3)	1.832(3)	Bi(5)–Bi(6)	1.847(3)	Bi(9)–Bi(10)	1.799(3)
–Bi(5)	1.842(3)	–Bi(9)	1.777(3)	–Bi(12)	1.829(3)
–Bi(7)	1.827(3)	–Bi(10)	1.745(3)	Bi(10)–Bi(11)	1.756(3)
–Bi(9)	1.864(3)	Bi(6)–Bi(10)	1.757(3)	–Bi(12)	1.735(3)
Bi(3)–Bi(4)	1.812(3)	–Bi(11)	1.793(3)	Bi(11)–Bi(12)	1.758(3)

B–B bond lengths within B_{12}(ii) icosahedron

Bii(1)–Bii(2)	1.818(3)	Bii(3)–Bii(7)	1.751(3)	Bii(7)–Bii(8)	1.810(3)
–Bii(3)	1.782(3)	–Bii(8)	1.784(3)	–Bii(9)	1.847(3)
–Bii(4)	1.786(3)	Bii(4)–Bii(6)	1.745(3)	–Bii(12)	1.856(3)
–Bii(5)	1.851(3)	–Bii(8)	1.768(3)	Bii(8)–Bii(11)	1.828(3)
–Bii(6)	1.753(3)	–Bii(11)	1.775(3)	–Bii(12)	1.790(3)
Bii(2)–Bii(3)	1.812(3)	Bii(5)–Bii(6)	1.849(3)	Bii(9)–Bii(10)	1.818(3)
–Bii(5)	1.878(3)	–Bii(9)	1.844(3)	–Bii(12)	1.857(3)
–Bii(7)	1.782(3)	–Bii(11)	1.782(3)	Bii(10)–Bii(11)	1.769(3)
–Bii(9)	1.860(3)	Bii(6)–Bii(10)	1.852(3)	–Bii(12)	1.799(3)
Bii(3)–Bii(4)	1.791(3)	–Bii(11)	1.767(3)	Bii(11)–Bii(12)	1.786(3)

B–B bond lengths within B_{12}(iii) icosahedron

Biii(1)–Biii(2)	1.804(3)	Biii(3)–Biii(7)	1.779(3)	Biii(7)–Biii(8)	1.827(3)
–Biii(3)	1.807(3)	–Biii(8)	1.773(3)	–Biii(9)	1.824(3)
–Biii(4)	1.774(3)	Biii(4)–Biii(6)	1.742(3)	–Biii(12)	1.866(3)
–Biii(5)	1.839(3)	–Biii(8)	1.797(3)	Biii(8)–Biii(11)	1.772(3)
–Biii(6)	1.742(3)	–Biii(11)	1.769(3)	–Biii(12)	1.740(3)
Biii(2)–Biii(3)	1.818(3)	Biii(5)–Biii(6)	1.792(3)	Biii(9)–Biii(10)	1.756(3)
–Biii(5)	1.861(3)	–Biii(9)	1.793(3)	–Biii(12)	1.800(3)
–Biii(7)	1.797(3)	–Biii(10)	1.732(3)	Biii(10)–Biii(11)	1.713(3)
–Biii(9)	1.808(3)	Biii(6)–Biii(10)	1.768(3)	–Biii(12)	1.745(3)
Biii(3)–Biii(4)	1.760(3)	–Biii(11)	1.777(3)	Biii(11)–Biii(12)	1.755(3)

B–B bond lengths within B_{12}(iv) icosahedron

Biv(1)–Biv(2)	1.840(3)	Biv(3)–Biv(7)	1.825(3)	Biv(7)–Biv(8)	1.829(3)
–Biv(3)	1.841(3)	–Biv(8)	1.800(3)	–Biv(9)	1.838(3)
–Biv(4)	1.793(3)	Biv(4)–Biv(6)	1.850(3)	–Biv(12)	1.818(3)
–Biv(5)	1.805(3)	–Biv(8)	1.810(3)	Biv(8)–Biv(11)	1.809(3)
–Biv(6)	1.848(3)	–Biv(11)	1.769(3)	–Biv(12)	1.835(3)
Biv(2)–Biv(3)	1.827(3)	Biv(5)–Biv(6)	1.880(3)	Biv(9)–Biv(10)	1.783(3)
–Biv(5)	1.823(3)	–Biv(9)	1.823(3)	–Biv(12)	1.863(3)
–Biv(7)	1.819(3)	–Biv(10)	1.853(3)	Biv(10)–Biv(11)	1.889(3)
–Biv(9)	1.843(3)	Biv(6)–Biv(10)	1.777(3)	–Biv(12)	1.811(3)
Biv(3)–Biv(4)	1.808(3)	–Biv(11)	1.771(3)	Biv(11)–Biv(12)	1.730(3)

TABLE V—*Continued*

B–B bond lengths within $B_{20}(C_2)$ unit

Bv(1)–Bv(2)	1.813(3)	Bv(4)–Bv(5)	1.831(3)	Bv(12)–Bv(13)	1.837(3)
–Bv(3)	1.812(3)	–Bv(9)	1.782(3)	–Bv(17)	1.778(3)
–Bv(4)	1.746(3)	–Bv(10)	1.794(3)	–Bv(19)	1.786(3)
–Bv(5)	1.857(3)	Bv(5)–Bv(6)	1.828(3)	Bv(13)–Bv(14)	1.862(3)
–Bv(12)	1.774(3)	–Bv(10)	1.785(3)	–Bv(17)	1.804(3)
–Bv(13)	1.825(3)	Bv(6)–Bv(7)	1.822(3)	Bv(14)–Bv(15)	1.846(3)
Bv(2)–Bv(3)	1.866(3)	–Bv(10)	1.834(3)	–Bv(17)	1.839(3)
–Bv(5)	1.735(3)	–Bv(11)	1.924(3)	–Bv(18)	1.909(3)
–Bv(6)	1.781(3)	Bv(7)–Bv(8)	1.820(3)	Bv(15)–Bv(16)	1.835(3)
–Bv(7)	1.848(3)	–Bv(11)	1.829(3)	–Bv(18)	1.856(3)
–Bv(15)	1.795(3)	–Bv(15)	1.976(3)	–Bv(20)	1.842(3)
–Bv(16)	1.736(3)	–Bv(20)	1.788(3)	Bv(16)–Bv(18)	1.808(3)
Bv(3)–Bv(7)	1.827(3)	Bv(8)–Bv(9)	1.888(3)	–Bv(19)	1.894(3)
–Bv(8)	1.748(3)	–Bv(11)	1.799(3)	Bv(17)–Bv(18)	1.815(3)
–Bv(13)	1.748(3)	Bv(9)–Bv(10)	1.726(3)	–Bv(19)	1.729(3)
–Bv(14)	1.788(3)	–Bv(11)	1.751(3)	Bv(18)–Bv(19)	1.799(3)
–Bv(15)	1.858(3)	Bv(10)–Bv(11)	1.840(3)		

B–B bond lengths within $B_{20}(C_s)$ unit

Bvi(1)–Bvi(2)	1.764(3)	Bvi(4)–Bvi(5)	1.831(3)	Bvi(10)–Bvi(11)	1.800(3)
–Bvi(3)	1.766(3)	–Bvi(9)	1.780(3)	–Bvi(12)	1.785(3)
–Bvi(4)	1.763(3)	–Bvi(10)	1.813(3)	Bvi(11)–Bvi(12)	1.781(3)
–Bvi(5)	1.823(3)	–Bvi(11)	1.795(3)	Bvi(13)–Bvi(17)	1.750(3)
–Bvi(9)	1.751(3)	Bvi(5)–Bvi(6)	1.824(3)	–Bvi(19)	1.842(3)
–Bvi(13)	1.742(3)	–Bvi(11)	1.808(3)	Bvi(14)–Bvi(15)	1.806(3)
Bvi(2)–Bvi(3)	1.876(3)	Bvi(6)–Bvi(7)	1.871(3)	–Bvi(17)	1.881(3)
–Bvi(5)	1.731(3)	–Bvi(11)	1.830(3)	–Bvi(18)	1.823(3)
–Bvi(6)	1.795(3)	–Bvi(12)	1.899(3)	Bvi(15)–Bvi(16)	1.802(3)
–Bvi(7)	1.813(3)	Bvi(7)–Bvi(8)	1.857(3)	–Bvi(18)	1.882(3)
–Bvi(14)	1.729(3)	–Bvi(12)	1.837(3)	–Bvi(20)	1.781(3)
–Bvi(15)	1.820(3)	–Bvi(15)	1.965(3)	Bvi(16)–Bvi(18)	1.890(3)
Bvi(3)–Bvi(7)	1.828(3)	–Bvi(20)	1.778(3)	–Bvi(19)	1.817(3)
–Bvi(8)	1.782(3)	Bvi(8)–Bvi(9)	1.850(3)	Bvi(17)–Bvi(18)	1.767(3)
–Bvi(9)	1.798(3)	–Bvi(10)	1.807(3)	–Bvi(19)	1.732(3)
–Bvi(15)	1.894(3)	–Bvi(12)	1.865(3)	Bvi(18)–Bvi(19)	1.773(3)
–Bvi(16)	1.772(3)	Bvi(9)–Bvi(10)	1.789(3)		

B–B bond lengths in the linkages B_{12}(i)–B_{12}(ii,iii,iv) and B_{12}(i)–$B_{20}(C_2,C_s)$

Bi(1)–Bii(7)	1.746(3)	Bi(5)–Bvi(20)	1.858(3)	Bi(9)–Bv(4)	1.715(3)
Bi(2)–Biv(5)	1.843(3)	Bi(6)–Bvi(17)	1.740(3)	Bi(10)–Biii(10)	1.602(3)
Bi(3)–Biii(8)	1.649(3)	Bi(7)–Bv(16)	1.758(3)	Bi(11)–Biv(3)	1.711(3)
Bi(4)–Bvi(11)	1.649(3)	Bi(8)–Bv(14)	1.864(3)	Bi(12)–Bii(1)	1.726(3)

B–B bond lengths in the linkages B_{12}(ii)–B_{12}(i,iii,iv) and B_{12}(ii)–$B_{20}(C_2,C_s)$

Bii(1)–Bi(12)	1.726(3)	Bii(5)–Bv(20)	1.869(3)	Bii(9)–Bvi(16)	1.821(3)
Bii(2)–Biv(2)	1.741(3)	Bii(6)–Bv(19)	1.751(3)	Bii(10)–Biv(11)	1.649(3)
Bii(3)–Biii(11)	1.650(3)	Bii(7)–Bi(1)	1.746(3)	Bii(11)–Biii(2)	1.763(3)
Bii(4)–Bv(10)	1.653(3)	Bii(8)–Bvi(4)	1.733(3)	Bii(12)–Bvi(14)	1.766(3)

TABLE V—*Continued*

B–B bond lengths in the linkages B_{12}(iii)–B_{12}(i,ii,iv) and B_{12}(iii)–B_{20}(C_2,C_s)

Biii(1)–Biv(12)	1.683(3)	Biii(5)–Bvi(20)	1.849(3)	Biii(9)–Bvi(13)	1.727(3)
Biii(2)–Bii(11)	1.763(3)	Biii(6)–Bv(9)	1.698(3)	Biii(10)–Bi(10)	1.602(3)
Biii(3)–Bv(17)	1.640(3)	Biii(7)–Bv(6)	1.863(3)	Biii(11)–Bii(3)	1.650(3)
Biii(4)–Bvi(10)	1.670(3)	Biii(8)–Bi(3)	1.649(3)	Biii(12)–Biv(1)	1.708(3)

B–B bond lengths in the linkages B_{12}(iv)–B_{12}(i,ii,iii) and B_{12}(iv)–B_{20}(C_2,C_s)

Biv(1)–Biii(12)	1.708(3)	Biv(5)–Bi(2)	1.843(3)	Biv(9)–Bvi(8)	1.751(3)
Biv(2)–Bii(2)	1.741(3)	Biv(6)–Bv(20)	1.914(3)	Biv(10)–Bv(12)	1.746(3)
Biv(3)–Bi(11)	1.711(3)	Biv(7)–Bv(8)	1.773(3)	Biv(11)–Bii(10)	1.649(3)
Biv(4)–Bvi(19)	1.730(3)	Biv(8)–Bvi(6)	1.914(3)	Biv(12)–Biii(1)	1.683(3)

B–B bond lengths in the linkages B_{20}(C_2)–B_{12} and B_{20}(C_2)–B_{20}(C_2,C_s)

Bv(1)[a]		Bv(8)–Biv(7)	1.773(3)	Bv(15)[a]	
Bv(2)[a]		Bv(9)–Biii(6)	1.698(3)	Bv(16)–Bi(7)	1.758(3)
Bv(3)[a]		Bv(10)–Bii(4)	1.653(3)	Bv(17)–Biii(3)	1.640(3)
Bv(4)–Bi(9)	1.715(3)	Bv(11)–Bvi(9)	1.720(3)	Bv(18)–Bv(5)	1.713(3)
Bv(5)–Bv(18)	1.713(3)	Bv(12)–Biv(10)	1.746(3)	Bv(19)–Bii(6)	1.751(3)
Bv(6)–Biii(7)	1.863(3)	Bv(13)–Bvi(12)	1.718(3)	Bv(20)–Bii(5)	1.869(3)
Bv(7)[a]		Bv(14)–Bi(8)	1.864(3)	–Biv(6)	1.914(3)

B–B bond lengths in the linkages B_{20}(C_s)–B_{12} and B_{20}(C_s)–B_{20}(C_2,C_s)

Bvi(1)[a]		Bvi(8)–Biv(9)	1.751(3)	Bvi(15)[a]	
Bvi(2)[a]		Bvi(9)–Bv(11)	1.720(3)	Bvi(16)–Bii(9)	1.821(3)
Bvi(3)[a]		Bvi(10)–Biii(4)	1.670(3)	Bvi(17)–Bi(6)	1.740(3)
Bvi(4)–Bii(8)	1.733(3)	Bvi(11)–Bi(4)	1.649(3)	Bvi(18)–Bvi(5)	1.705(3)
Bvi(5)–Bvi(18)	1.705(3)	Bvi(12)–Bv(13)	1.718(3)	Bvi(19)–Biv(4)	1.730(3)
Bvi(6)–Biv(8)	1.914(3)	Bvi(13)–Biii(9)	1.727(3)	Bvi(30)–Bi(5)	1.858(3)
Bvi(7)[a]		Bvi(14)–Bii(12)	1.766(3)	–Biii(5)	1.849(3)

[a] This atom is not bonded to boron atoms outside the unit to which it belongs.

same direction as Fig. 2 or Fig. 3. The arrangement has alternate zigzag chains of the two units running infinitely in the direction of the *c* axis. The B_{20} units occupy all of the B_{144}-(T_d) truncated tetrahedral holes in the B_{12} icosahedral arrangement; the sequence of the B_{20} units in the figure is consistent with that of the truncated tetrahedra in Fig. 3. Each linkage between the B_{20} units is made across a hexagonal plane shared between the truncated tetrahedral holes accommodating these units. As every truncated tetrahedral hole has four such hexagonal faces shared with four similar holes (Fig. 3), each B_{20} unit in the truncated tetrahedral hole is linked to four B_{20} units (2B_{20}-(C_2), 2B_{20}-(C_s)) in the four neighboring holes. Thus, each of the B_{20} units is tetrahedrally coordinated with four B_{20} units. Three of the linkages of each B_{20} unit with the surrounding B_{20} units are seen in Fig. 4, and the fourth linkage approximately vertical to the projection plane of the figure, is seen in Fig. 5.

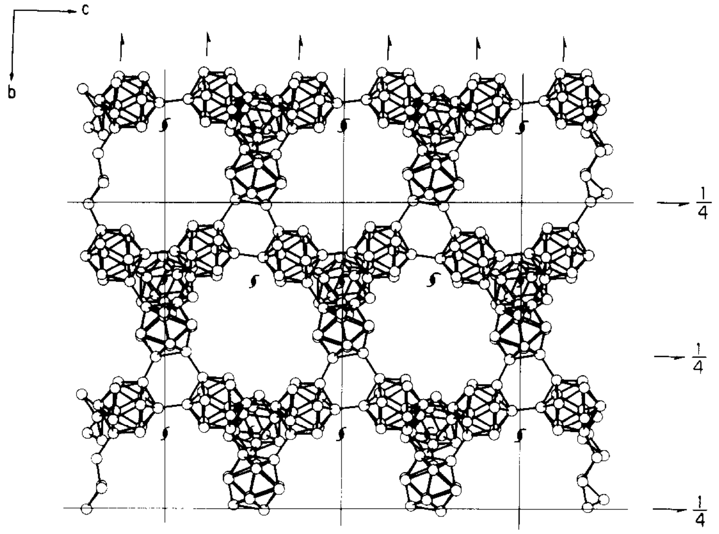

FIG. 2. B_{12} icosahedral arrangement in a view parallel to [100] ($0.14 < x < 0.64$).

In the B_{12} icosahedral framework (Figs. 2 and 3), every B_{12} icosahedron is surrounded by six B_{12} icosahedra and is shared among six B_{144}-(T_d) truncated tetrahedra. Thus, the six apical atoms of the icosahedron are used for bonding to the six surrounding B_{12} units and six remaining apical atoms are provided for the linkages to six B_{20} units

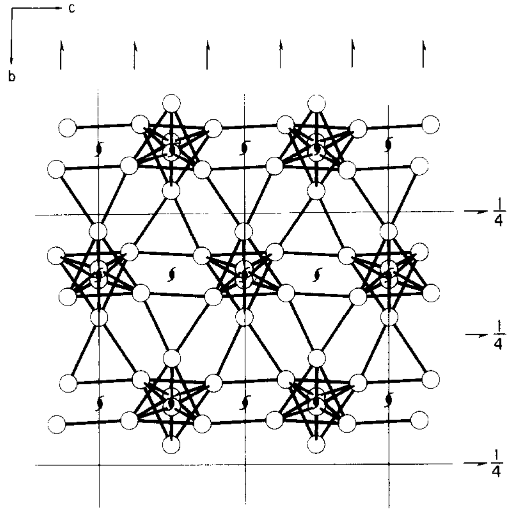

FIG. 3. Arrangement of the B_{48}-(T_d) subunit as seen along the a axis, showing B_{144}-(T_d) truncated tetrahedral holes. The circles represent B_{12} icosahedra.

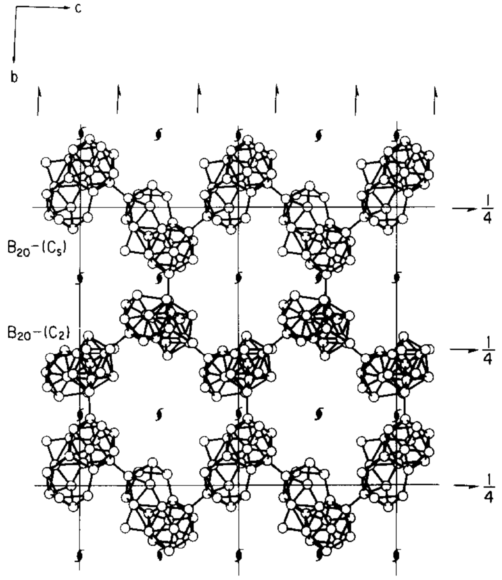

FIG. 4. Arrangement of B_{20} units in a view parallel to [100] ($0 < x < 0.5$).

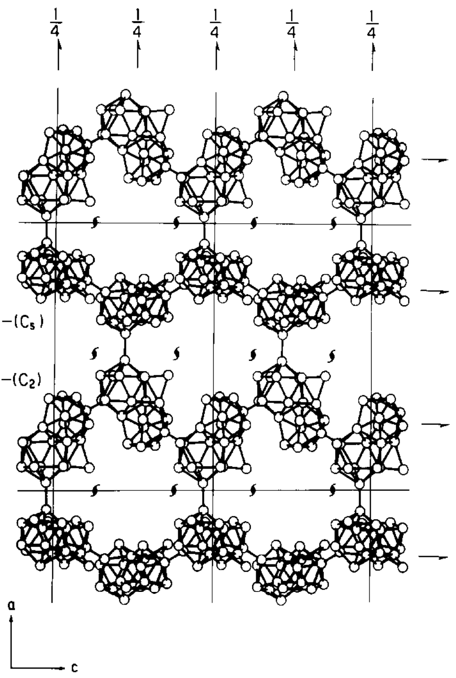

FIG. 5. Arrangement of B_{20} units in a view parallel to [010] ($0.25 < y < 0.75$).

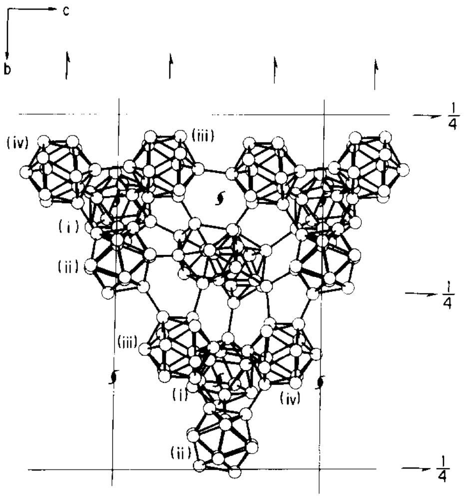

FIG. 6. Features of the linkages between a B_{20}-(C_2) unit and B_{12} icosahedra as seen along the *a* axis.

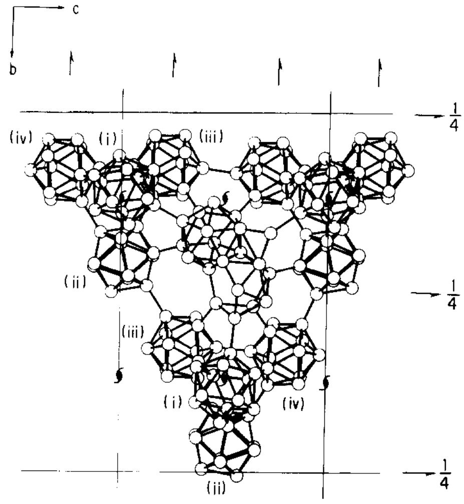

FIG. 7. Features of the linkages between a B_{20}-(C_s) unit and B_{12} icosahedra as seen along the *a* axis.

($3B_{20}$-(C_2), $3B_{20}$-(C_s)), because, as described above, every truncated tetrahedron B_{144}-(T_d) accommodates a B_{20}-(C_2) or B_{20}-(C_s) unit. On the other hand, the B_{20}-(C_2) or B_{20}-(C_s) unit in the B_{144}-(T_d) truncated icosahedron is linked to the 12 apical B_{12} icosahedra and four B_{20} units ($2B_{20}$-(C_2), $2B_{20}$-(C_s)). In other words, 12 B_{12} are enclosing every B_{20} unit in a truncated tetrahedral form, and four B_{20} units surround it tetrahedrally. Owing to their positions in the unit, five of the twenty boron atoms of each B_{20}-(C_2) or B_{20}-(C_s) unit are bonded to none of the atoms belonging to separate boron units. On the other hand, one atom of the remaining 15 boron atoms, which corresponds to B(23) in α-AlB_{12} (*8*), lying at a special site, is bonded to two atoms, each of which belongs to a different boron unit. Consequently, both B_{20}-(C_2) and B_{20}-(C_s) units have the coordination number of 16. The linkages between B_{20}-(C_2) and B_{12} units are presented in Fig. 6, and those between B_{20}-(C_s) and B_{12} units are shown in Fig. 7. In both figures, the arrangements of the B_{12} icosahedra are identical, except that the B_{12}(i) units in one figure are related to the B_{12}(i) units in the other by twofold screw axes located at the centers of the B_{48}-(T_d) subunits parallel to the *a* axis. Although a total of 12 icosahedra is actually linked to

TABLE VI

THE RANGES AND AVERAGE VALUES OF B–B BOND LENGTHS WITHIN OR BETWEEN BORON STRUCTURAL SUBUNITS

B–B bond lengths (Å)	Number	Range of lengths	Average length
Within units			
B_{12}(i)	30	1.735(3)–1.864(3)	1.804
B_{12}(ii)	30	1.745(3)–1.878(3)	1.806
B_{12}(iii)	30	1.713(3)–1.866(3)	1.784
B_{12}(iv)	30	1.730(3)–1.889(3)	1.820
$B_{20}(C_2)$	50	1.726(3)–1.976(3)	1.816
$B_{20}(C_s)$	50	1.729(3)–1.965(3)	1.811
Between units			
B_{12}(i)–B_{12}, B_{20}	12	1.602(3)–1.864(3)	1.738
B_{12}(ii)–B_{12}, B_{20}	12	1.649(3)–1.869(3)	1.739
B_{12}(iii)–B_{12}, B_{20}	12	1.602(3)–1.863(3)	1.709
B_{12}(iv)–B_{12}, B_{20}	12	1.649(3)–1.914(3)	1.764
$B_{20}(C_2)$–B_{12}, B_{20}	16	1.640(3)–1.914(3)	1.757
$B_{20}(C_s)$–B_{12}, B_{20}	16	1.649(3)–1.914(3)	1.754

each B_{20} unit, three icosahedra overlapping the B_{20} unit are omitted in these figures. The three icosahedra, being linked in a triangular form, coordinate to a B_{20} unit from the lower side of the unit (B_{20}-(C_2) in Fig. 6) or the supper side of the unit (B_{20}-(C_s) in Fig. 7) so as to have its triangular plane parallel to the plane of projection. The B_{20}-(C_2) and B_{20}-(C_s) units, located at positions as in Figs. 6 and 7, respectively, are directly bonded to each other. It is the linkage of B_{20}-(C_2) and B_{20}-(C_s) in the direction of the *a* axis (Fig. 5), which is referred to above as the fourth linkage between B_{20} units. As in the case of α-AlB_{12} (*8*), there is only one linkage (two-center B–B bond (*12*)) between every two adjacent boron structural subunits, and all the linkages form approximately along the pseudo-five-fold axes of the icosahedra or along similar directions in the B_{20} units (Figs. 2, 4–7). In Table VI, the B–B bond lengths in the boron framework are tabulated. As is seen in other B_{12} icosahedral or α-AlB_{12} type crystals, the B–B bond lengths in the linkages B_{12}–B_{12}, B_{12}–B_{20}, and B_{20}–B_{20} are, on the whole, appreciably shorter than those within the structural subunits.

The Distribution of the Aluminum Atoms

The aluminum atoms are distributed among 11 sites. As in α-AlB_{12} and the other relevant compounds, AlB_{10} (*13*) and C_4AlB_{24} (*14*) or $C_8Al_{2.1}B_{51}$ (*15*), none of the Al sites is fully occupied (Table III). In Table VII, the distances between the Al sites and their respective boron first neighbors are presented. The nature of the coordinations of the boron atoms about the Al sites is demonstrated stereoscopically in Fig. 8. As seen from the table or the figure, each of the sites is enclosed by 10 to 14 boron atoms. The distances vary within relatively wide ranges. However, as in the case of α-AlB_{12} (*8*), the boron first neighbors are distinguishable from the second neighbors. The five shortest distances, Al(1)–Bvi(17), Al(6,10)–Bv(19), and Al(7,8)–Bv(9), ranging from 2.03 to 2.09 Å, are appreciably shorter than the sum of the covalent Al radii and the average B radii in B–B bonds within the B_{12} and B_{20} units 1.26 (*16*) and 0.904 Å. The two boron atoms Bv(19) and Bv(9), to which the Al(6,10) and Al(7,8) are considered to be strongly bonded, are apical atoms of the separate open pentagonal faces of B_{20}-(C_2) unit. The situation is just the same as in α-AlB_{12}. The B(14) and B(14′) atoms of B_{20}-(C_2) in α-AlB_{12} (*8*, *12*), to which Al atoms are bonded with short distances (B(14,14′)–Al(1): 2.079 Å and B(14,14′)–Al(3): 2.043 Å) (*8*), are equivalent to the Bv(19) and Bv(9) of the present crystal with respect to their positions at the open pentagonal apexes. In the same way, Bvi(17) of B_{20}-(C_s), to which Al(1) is bonded with a short distance, corresponds to Bv(9,19) of B_{20}-(C_2) (or B(14,14′) in α-AlB_{12}) with respect to its position. The short distances described thus far suggest that, as in the case of α-AlB_{12}, relatively

TABLE VII

Distances between Al and B First Neighbors[a]

Al(1)–Bvi(17)	2.083(2)	Al(4)–Bvi(16)^{1}	2.469(3)	Al(8)–Bvi(6)^{1}	2.357(3)
–Bi(5)	2.210(2)	–Bii(5)^{3}	2.471(3)	–Bvi(20)^{1}	2.396(3)
–Bii(7)^{3}	2.263(2)	–Bv(11)^{9}	2.483(3)	–Bv(13)^{6}	2.488(3)
–Bi(6)	2.286(2)	–Bv(20)^{8}	2.756(3)	–Bv(3)^{6}	2.561(3)
–Bvi(15)^{1}	2.303(3)	Al(5)–Bv(1)	2.189(3)	–Bv(1)	2.566(3)
–Bii(9)^{3}	2.306(3)	–Bi(2)	2.244(2)	–Biii(6)	2.690(3)
–Bvi(16)^{1}	2.322(2)	–Bv(12)	2.268(3)	–Biii(5)	2.703(3)
–Bvi(20)^{1}	2.330(2)	–Biv(5)^{3}	2.277(3)	–Biv(8)^{10}	2.800(3)
–Bi(1)	2.343(2)	–Bv(16)	2.337(3)	Al(9)–Bi(2)	2.226(4)
–Bvi(14)^{4}	2.416(2)	–Bi(7)	2.349(3)	–Bv(1)	2.236(4)
–Bii(12)^{3}	2.485(2)	–Bv(4)	2.374(3)	–Biv(5)^{3}	2.253(4)
–Bvi(13)	2.828(2)	–Bi(9)	2.388(3)	–Bv(4)	2.318(4)
–Bvi(18)^{1}	2.920(2)	–Bv(15)	2.439(3)	–Bvi(8)^{1}	2.368(4)
Al(2)–Bvi(1)	2.201(2)	–Biv(10)^{3}	2.440(3)	–Bvi(7)^{1}	2.380(4)
–Bvi(13)	2.215(2)	–Bv(5)	2.516(3)	–Bi(9)	2.380(4)
–Biii(2)	2.218(2)	–Bv(18)	2.554(3)	–Biv(9)^{3}	2.399(4)
–Bii(11)^{5}	2.224(2)	–Biv(6)^{3}	2.583(3)	–Bv(12)	2.415(4)
–Bvi(14)	2.277(2)	–Bv(20)	2.842(3)	–Bi(5)	2.454(4)
–Biii(9)	2.292(2)	Al(6)–Bv(19)^{6}	2.087(3)	–Biv(10)^{3}	2.494(4)
–Bii(12)^{5}	2.357(2)	–Bi(12)^{6}	2.231(3)	–Bv(13)^{6}	2.495(4)
–Bvi(15)^{1}	2.377(2)	–Bi(8)^{6}	2.242(3)	–Bvi(12)^{1}	2.522(4)
–Bii(8)^{5}	2.400(2)	–Bii(1)^{6}	2.280(2)	–Bvi(20)^{1}	2.708(4)
–Bvi(4)	2.423(2)	–Bii(5)^{6}	2.300(3)	Al(10)–Bv(19)^{6}	2.031(5)
–Biii(5)	2.507(2)	–Bv(14)	2.304(3)	–Bv(15)	2.100(5)
–Bvi(18)^{1}	2.543(2)	–Bii(6)^{6}	2.317(3)	–Bv(12)	2.201(5)
–Bvi(5)	2.553(2)	–Bv(15)	2.351(3)	–Bv(18)	2.219(5)
–Bvi(20)^{1}	2.785(2)	–Bv(16)^{6}	2.385(3)	–Bv(16)^{6}	2.257(5)
Al(3)–Bvi(19)^{6}	2.131(2)	–Bv(20)	2.405(3)	–Bv(5)	2.332(5)
–Biv(6)^{6}	2.214(2)	–Bi(7)^{6}	2.495(3)	–Bv(1)	2.405(5)
–Biii(7)^{6}	2.231(2)	Al(7)–Bv(9)	2.050(3)	–Bv(2)	2.457(5)
–Bvi(13)^{6}	2.234(2)	–Biii(5)	2.224(3)	–Bv(14)	2.460(5)
–Bv(6)^{7}	2.289(2)	–Bvi(6)^{1}	2.238(3)	–Bv(20)	2.549(5)
–Biii(12)^{6}	2.296(2)	–Biv(8)^{10}	2.271(3)	Al(11)–Biv(7)^{6}	2.225(9)
–Bv(20)^{2}	2.335(3)	–Biii(6)	2.309(3)	–Bii(5)^{6}	2.240(9)
–Bv(7)^{2}	2.351(2)	–Bv(8)^{6}	2.312(3)	–Biv(3)^{6}	2.264(9)
–Biv(4)^{6}	2.359(2)	–Bvi(7)^{1}	2.357(3)	–Bi(11)^{6}	2.290(9)
–Biii(9)^{6}	2.361(2)	–Bvi(20)^{1}	2.373(3)	–Bii(1)^{6}	2.295(9)
–Biv(1)^{6}	2.378(2)	–Biii(1)	2.475(3)	–Bv(8)	2.317(9)
Al(4)–Bv(8)^{8}	2.269(3)	–Biv(12)^{10}	2.499(3)	–Bii(2)^{6}	2.324(9)
–Biv(7)^{3}	2.278(3)	–Biv(7)^{10}	2.576(3)	–Bi(8)^{6}	2.367(9)
–Bii(2)^{3}	2.289(3)	–Bvi(12)^{1}	2.769(3)	–Bi(12)^{6}	2.39(1)
–Bvi(3)^{1}	2.297(3)	–Bv(4)	2.796(3)	–Biv(2)^{6}	2.426(9)
–Biv(2)^{3}	2.302(3)	Al(8)–Bv(9)	2.027(3)	–Bv(3)	2.473(9)
–Biv(9)^{3}	2.394(3)	–Bvi(7)^{1}	2.147(3)	–Bv(14)	2.559(9)
–Bv(7)^{8}	2.409(3)	–Bv(4)	2.283(3)	–Bv(20)	2.646(9)
–Bii(9)^{3}	2.435(3)	–Bv(8)^{6}	2.288(3)	–Bv(7)	2.69(1)
–Bvi(9)^{6}	2.439(3)	–Bvi(12)^{1}	2.292(3)	–Bv(15)	2.875(9)
–Bvi(8)^{1}	2.461(3)				

---

[a] The atomic sites are designated with the following symmetry codes: none (x, y, z), $1(\frac{1}{2} - x, -y, \frac{1}{2} + z)$, $2(-x, \frac{1}{2} + y, \frac{1}{2} - z)$, $3(-\frac{1}{2} + x, \frac{1}{2} - y, -z)$, $4(\frac{1}{2} - x, -y, -\frac{1}{2} + z)$, $5(1 - x, -\frac{1}{2} + y, \frac{1}{2} - z)$, $6(\frac{1}{2} - x, 1 - y, \frac{1}{2} + z)$, $7(-\frac{1}{2} + x, \frac{3}{2} - y, 1 - z)$, $8(-x, -\frac{1}{2} + y, \frac{1}{2} - z)$, $9(-\frac{1}{2} + x, \frac{1}{2} - y, 1 - z)$, and $10(x, y, 1 + z)$.

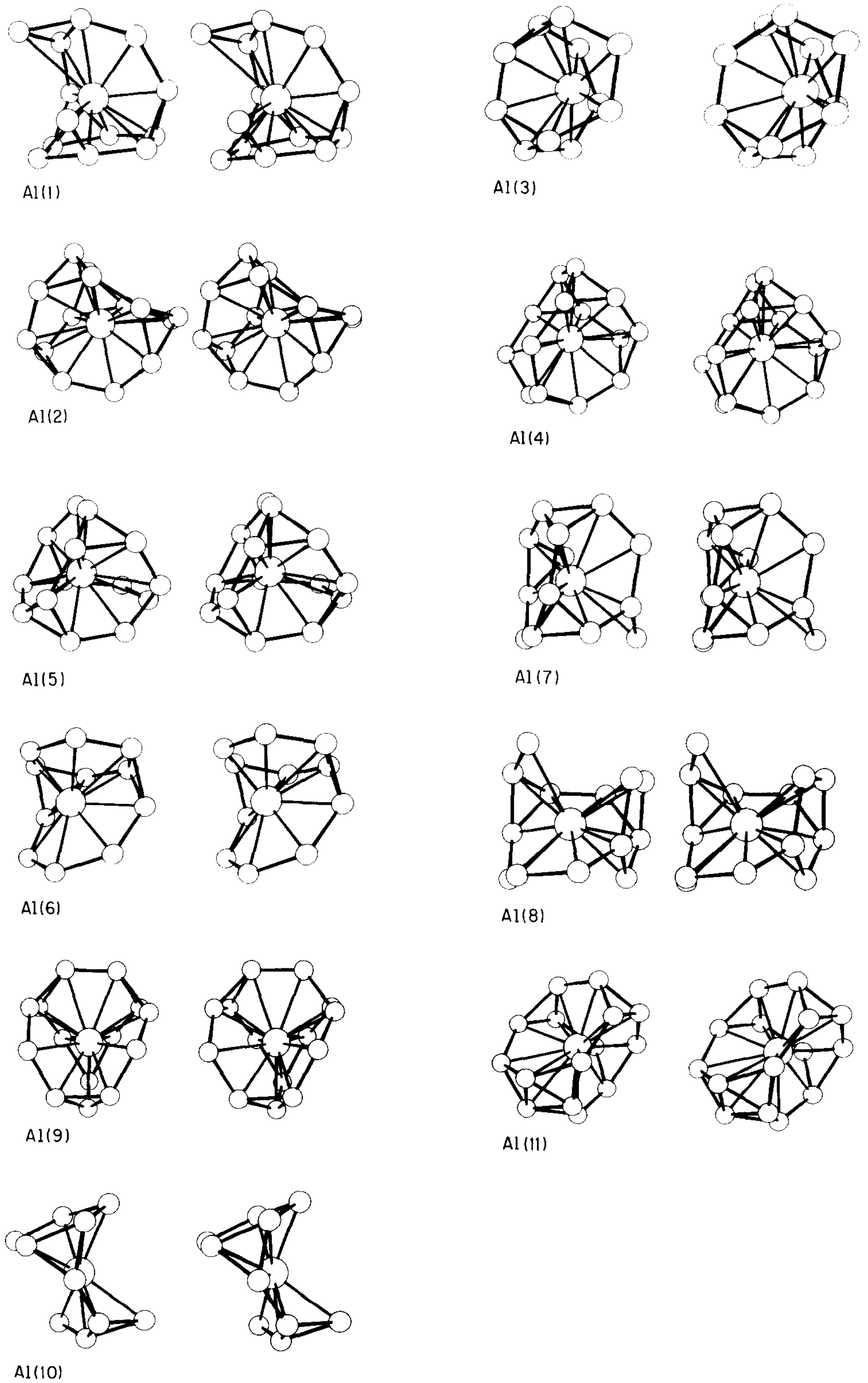

FIG. 8. Stereoscopic drawings demonstrating the coordination of Al sites as seen along the *a* axis. The direction connecting the two central Al atoms in each figure is parallel to the *c* axis; the axis is directed toward the right side of the figure.

TABLE VIII

Al–Al DISTANCES WITH UNUSUALLY SHORT INTERVALS

Sites	Occupancies	Distances (Å)
Al(4)–Al(11)	0.52–0.07	2.417(9)
Al(5)–Al(9)	0.75–0.19	2.136(4)
–Al(10)	0.75–0.19	2.238(5)
Al(6)–Al(10)	0.76–0.19	1.186(5)
–Al(11)	0.76–0.07	2.257(9)
Al(7)–Al(8)	0.51–0.44	0.786(3)
Al(8)–Al(9)	0.44–0.19	2.373(4)

strong interactions between Al and the B_{20} units are present through the apical atoms of the open pentagonal faces; as to B_{20}-(C_2) in α-AlB_{12}, some indications of such interaction are manifested in the X-ray difference electron densities (*12*).

In Table VIII, Al site pairs having distances shorter than two times the covalent Al radii 2.52 Å are given, together with the occupancies of the sites. Owing to the unusually short distances, simultaneous occupation of the two sites of each of the pairs is impossible. Accordingly, the sum of the occupancies of the Al site pair should, in every case, be less than 100%. As seen from the occupation data in the table, this requirement is fulfilled. However, the significant variations in the sums of occupancies, 59 to 96%, obviously arise from some other structural requirements. Therefore, the varying occupancies of the 11 Al site (Table III), 7 to 96%, which result in variations of the sums of occupancies of the Al site pairs, are expected to stabilize the boron framework of this compound. The results of further examination and detailed discussions on this subject will be given in the next subsection.

Charge Balance among Boron Structural Subunits

In a previous work (*7*), the author examined the nature of the metal distribution in the crystals of α-AlB_{12} structure type, and introduced the idea of "charge balance" between B_{12} and B_{20} (B_{20}-(C_2)) units, suggesting the validity of the ionic formula 10/3 $Al^{+3} \cdot 2B_{12}^{-2} \cdot B_{20}^{-6}$ (*12*). In those crystals (α-AlB_{12} and four different crystals with the composition $Al_{\sim1.1}Be_{\sim0.6}B_{22}$), despite significant variations in metal distribution, the metallic valence electron numbers allotted to the B_{12} and B_{20} in proportion to the frequencies in the contacts of the units with metals were, in every case, ~2 and ~5.5, respectively. Accordingly, it was inferred that the metal distributions in the crystals of this type occur so as to preserve a negative charge balance between B_{12} and B_{20} in the ratio of about 1 : 3, which is presumably essential to make up the stable boron framework.

The procedure of allotting the metallic valance electrons to the boron structural subunits, which has been applied to the present crystal, is the same as in a previous publication (*7*). All the valence electrons of the metals are regarded as contributing equally to the stabilization of the boron framework. Thus, Z/N valence electrons are allotted to every metal–boron contact, where Z and N are the number of the valence electrons and the coordination number of the metal, respectively. The sum of the Z/N values over all the boron atoms within each of the structural subunits and over all the metals concerned is the total number of the electrons of the unit.

According to preliminary molecular orbital calculations, the B_{20}-(C_s) unit, in the same manner as B_{20}-(C_2) (*12*), needs −6 charges to attain a stable electronic configuration (*17*). Consequently, by analogy with the case of α-AlB_{12} (*12*), the ionic formula 20/3 $Al^{+3} \cdot 4B_{12}^{-2} \cdot 2B_{20}^{-6}$ may be assigned to γ-AlB_{12}. Thus, if the ionic formula for α-AlB_{12} or the idea of the charge balance in the boron structures of α-AlB_{12} type is chemically reasonable, the sums of the Z/N

TABLE IX

ALLOTMENT OF METALLIC VALENCE ELECTRONS TO B_{12}(i, ii, iii, iv) AND B_{20}-(C_2,C_s)[a]

Al(j)	Al(1)	Al(2)	Al(3)	Al(4)	Al(5)	Al(6)	Al(7)	Al(8)	Al(9)	Al(10)	Al(11)	$\sum_j (Z \cdot f_{ij}/N_j)$
P_j	0.96	0.95	0.95	0.52	0.75	0.76	0.51	0.44	0.19	0.19	0.07	
$N_j = \sum_i n_{i,j}$	13	14	11	14	14	11	13	13	14	10	15	
$n_{1,j}$	3	0	0	0	3	3	0	0	3	0	3	
$n_{2,j}$	3	3	0	3	0	3	0	0	0	0	3	
$n_{3,j}$	0	3	3	0	0	0	3	2	0	0	0	
$n_{4,j}$	0	0	3	3	3	0	3	1	3	0	3	
$n_{5,j}$	0	0	3	4	8	5	3	6	4	10	6	
$n_{6,j}$	7	8	2	4	0	0	4	4	4	0	0	
$f_{1,j}$	2.88	0	0	0	2.25	2.28	0	0	0.57	0	0.21	
$f_{2,j}$	2.88	2.85	0	1.56	0	2.28	0	0	0	0	0.21	
$f_{3,j}$	0	2.85	2.85	0	0	0	1.53	0.88	0	0	0	
$f_{4,j}$	0	0	2.85	1.56	2.25	0	1.53	0.44	0.57	0	0.21	
$f_{5,j}$	0	0	2.85	2.08	6.00	3.80	1.53	2.64	0.76	1.90	0.42	
$f_{6,j}$	6.72	7.60	1.90	2.08	0	0	2.04	1.76	0.76	0	0	
$Z \cdot f_{1,j}/N_j$	0.66	0	0	0	0.48	0.62	0	0	0.12	0	0.04	1.9
$Z \cdot f_{2,j}/N_j$	0.66	0.61	0	0.33	0	0.62	0	0	0	0	0.04	2.2
$Z \cdot f_{3,j}/N_j$	0	0.61	0.78	0	0	0	0.35	0.20	0	0	0	1.9
$Z \cdot f_{4,j}/N_j$	0	0	0.78	0.33	0.48	0	0.35	0.10	0.12	0	0.04	2.2
$Z \cdot f_{5,j}/N_j$	0	0	0.78	0.45	1.29	1.04	0.35	0.61	0.16	0.57	0.08	5.3
$Z \cdot f_{6,j}/N_j$	1.55	1.63	0.52	0.45	0	0	0.47	0.41	0.16	0	0	5.2

α-AlB$_{12}$[b]

Al(j)	Al(1)	Al(2)	Al(3)	Al(4)	Al(5)	$\sum_j (Z \cdot f_{ij}/N_j)$
P_j	0.72	0.49	0.24	0.15	0.02	
$N_j = \sum_i n_{i,j}$	11	13	10	12	10	
$n_{1,j}$	6	6	0	9	3	
$n_{2,j}$	5	7	10	3	7	
$f_{1,j}$	4.32	2.94	0	1.35	0.06	
$f_{2,j}$	7.20	2.51	4.80	0.90	0.28	
$Z \cdot f_{1,j}/N_j$	1.18	0.68	0	0.34	0.02	2.2
$Z \cdot f_{2,j}/N_j$	1.97	1.58	1.44	0.24	0.08	5.3

[a] The subscripts 1, 2, 3, 4, 5, and 6 of n or f refer to boron atoms in B_{12}(i), B_{12}(ii), B_{12}(iii), B_{12}(iv), B_{20}-(C_2), and B_{20}-(C_s), respectively.

[b] The subscripts 1 and 2 of n or f refer to boron atoms in B_{12} and B_{20} units, respectively.

values for B_{12}(i,ii,iii,iv), B_{20}-(C_2), and B_{20}-(C_s) in the present crystal also should be approximately 2, 6, and 6, respectively; the boron structural subunits constructing α-AlB$_{12}$ are just the same as those in γ-AlB$_{12}$, excepting for the small structural difference between B_{20}-(C_2) and B_{20}-(C_s).

In Table IX, the numbers of the metallic valence electrons allotted to the six boron structural subunits are presented, together with the data from which the final values are derived. The corresponding data of α-AlB$_{12}$ (*7*) are also given for comparison in this table. As in the case of α-AlB$_{12}$, the Al atoms are taken as being in contact with their respective B first neighbors (Table VII). The number of valence electrons Z is three for Al, $n_{i,j}$ is the number of the coordination of B for the ith boron unit about Al(j), and N_j is the total coordination number of B about Al(j). The $f_{i,j}$ is the frequency of contact of Al(j) with the ith unit; it is obtained by multiplying $n_{i,j}$ by the occupancy of Al(j), P_j. The value $Z \cdot f_{i,j}/N_j$ is the number of the valence electrons of Al(j) allotted to the ith boron unit. The $\sum_j Z \cdot f_{i,j}/N_j$, which is the sum of $Z \cdot f_{i,j}/N_j$ over all the aluminum sites concerned, is the total number of the valence electrons allotted to the ith unit.

The results of the examination are summarized in the following.

(1) The numbers of the metallic valence electrons allotted to the four B_{12} units are almost equal (2.05 ± 0.15), and in good agreement with the value assigned for B_{12} in α-AlB_{12}.

(2) The number of the valence electrons for B_{20}-(C_2), 5.3, is equal to the value for B_{20}-(C_2) in α-AlB_{12}.

(3) The number of the valence electrons for B_{20}-(C_s), 5.2, is almost equal to the value for B_{20}-(C_s).

In contrast to the complicated distributions and wide variances in the occupancies of the Al sites, the results of the charge assignments are compatible with the simple ionic formula $20/3\ Al^{+3} \cdot 4B_{12}{}^{-2} \cdot 2B_{20}{}^{-6}$ proposed from molecular orbital calculations. Further, considering that the arrangements of the boron units in the present crystal are quite different from those in α-AlB_{12}, the excellent agreement between the final values for the different phases is noteworthy.

The number of valence electrons allotted to the B_{20} units, 5.3 or 5.2, is somewhat less than that assigned in the proposed ionic formula $20/3\ Al^{+3} \cdot 4B_{12}{}^{-2} \cdot 2B_{20}{}^{-6}$. However, considering the relatively strong interactions between Al and these units, as described in the preceding subsection, the number of electrons to be allotted to the B_{20} units might be somewhat greater than those given in the table. It is of interest that the chemical composition of the present crystal $AlB_{13.97}$ obtained by structure analysis, as well as that of α-AlB_{12}, $AlB_{13.75}$ (*8*), is much closer to the composition $AlB_{13.2}$ derived from the ionic formula than to the formal composition AlB_{12}.

From what has been described so far, both the ionic formulae proposed for γ-AlB_{12} and α-AlB_{12} seem to have chemical significance. Even though the actual electron transfer from Al to the boron framework may be much smaller due to back donation, there should be a negative charge balance between B_{12} and B_{20} units at a ratio of about 1 : 3, which is presumably essential for making up the stable boron framework of the two phases. It is convincing that two different ways of charge assignment, i.e., the examination of the contact frequencies between Al and B units and the molecular orbital calculations, give compatible results.

Acknowledgment

The author is indebted to Dr. T. Ito for use of his unpublished molecular orbital data on the $B_{20}0(C_s)$ unit, and also gratefully acknowledges helpful discussions on this work.

References

1. I. HIGASHI AND Y. TAKAHASHI, *J. Less Common Met.* **81,** 135 (1981).

2. J. A. KOHN AND D. W. ECKART, *Z. Kristallogr.* **116,** 134 (1961).

3. J. A. KOHN, *in* "Boron: Synthesis, Structure, and Properties" J. A. Kohn, W. F. Nye, and G. K. Gaulé (Eds.), pp. 75–82. Plenum, New York, 1960.

4. A. A. GIARDINI, J. A. KOHN, L. TOMAN, AND D. W. ECKART, *in* "Boron: Synthesis, Structure, and Properties" J. A. Kohn, W. F. Nye, and G. K. Gaulé (Eds.), pp. 140–158, Plenum, New York, 1960.

5. V. I. MATKOVICH, J. ECONOMY, AND R. F. GIESE, JR., *J. Amer. Chem. Soc.* **86,** 2337 (1964).

6. R. E. HUGHES, M. E. LEONOWICZ, J. T. LEMLEY, AND L.-T. TAI, *J. Amer. Chem. Soc.* **99,** 5507 (1977).

7. I. HIGASHI, *J. Solid State Chem.* **32,** 201 (1980).
8. I. HIGASHI, T. SAKURAI, AND T. ATODA, *J. Solid State Chem.* **20,** 67 (1977).
9. J. S. KASPER, M. VLASSE, AND R. NASLAIN, *J. Solid State Chem.* **20,** 281 (1977).
10. "International Tables for X-ray Crystallography," Vol. IV, pp. 72–74, Kynoch Press, Birmingham, England (1974).
11. T. SAKURAI AND K. KOBAYASHI, *Rep. Inst. Phys. Chem. Res. Tokyo* **55,** 69 (1979).
12. T. ITO, I. HIGASHI, AND T. SAKURAI, *J. Solid State Chem.* **28,** 171 (1979).
13. G. WILL, *Acta Crystallogr.* **23,** 1071 (1967).
14. G. WILL, *Acta Crystallogr.* **B25,** 1219 (1969).
15. A. J. PERROTTA, W. D. TOWNES, AND J. A. POTENZA, *Acta Crystallogr.* **B25,** 1223 (1969).
16. L. PAULING AND M. L. HUGGINS, *Z. Kristallogr.* **87,** 205 (1934).
17. T. ITO, private communication.